Structure and Composition Analysis of Natural Gas Hydrates: ^{13}C NMR Spectroscopic and Gas Uptake Measurements of Mixed Gas Hydrates

Yutaek Seo

CSIRO Petroleum Resources, 26 Dick Perry Avenue, Kensington, Perth, WA 6151, Australia

Seong-Pil Kang*

Clean Fossil Energy Research Center, Korea Institute of Energy Research, 102 Gajeongro, Yuseong-gu, Daejeon 305-343, Republic of Korea

Wonho Jang

Department of Environmental Engineering, Kyoungpook National University, 1370 Sankyuk-dong, Daegu 702-701, Republic of Korea

Received: May 28, 2009; Revised Manuscript Received: July 15, 2009

Gas hydrates are becoming an attractive way of storing and transporting large quantities of natural gas, although there has been little effort to understand the preferential occupation of heavy hydrocarbon molecules in hydrate cages. In this work, we present the formation kinetics of mixed hydrate based on a gas uptake measurement during hydrate formation, and how the compositions of the hydrate phase are varied under corresponding formation conditions. We also examine the effect of silica gel pores on the physical properties of mixed hydrate, including thermodynamic equilibrium, formation kinetics, and hydrate compositions. It is expected that the enclathration of ethane and propane is faster than that of methane early stage hydrate formation, and later methane becomes the dominant component to be enclathrated due to depletion of heavy hydrocarbons in the vapor phase. The composition of the hydrate phase seems to be affected by the consumed amount of natural gas, which results in a variation of heating value of retrieved gas from mixed hydrates as a function of formation temperature. ^{13}C NMR experiments were used to measure the distribution of hydrocarbon molecules over the cages of hydrate structure when it forms either from bulk water or water in silica gel pores. We confirm that 70% of large cages of mixed hydrate are occupied by methane molecules when it forms from bulk water; however, only 19% of large cages of mixed hydrate are occupied by methane molecules when it forms from water in silica gel pores. This result indicates that the fractionation of the hydrate phase with heavy hydrocarbon molecules is enhanced in silica gel pores. In addition when heavy hydrocarbon molecules are depleted in the vapor phase during the formation of mixed hydrate, structure I methane hydrate forms instead of structure II mixed hydrate and both structures coexist together, which is also confirmed by ^{13}C NMR spectroscopic analysis.

Introduction

Gas hydrates, also known as clathrate hydrates, are nonstoichiometric crystalline compounds formed when "guest" molecules of suitable size and shape are incorporated into a lattice structure built by the hydrogen-bonded "host" water molecules. Three distinct structural families, termed structures I, II, and H, are known, showing distinct size and shape of polyhedral cages that capture the guest molecules according to the structures.[1] Gas hydrates have been a particular concern of the oil and gas industry because the operating conditions of oil and gas production pipelines may be favorable to the formation of gas hydrate, resulting in blockage of pipelines.[2] However, the studies of gas hydrate have greatly evolved because of not only the concern in production pipelines but also the great potential of hydrates as a source of natural gas as there are massive deposits both under the permafrost and in the sediment of the continental margins.[3−5] Gas hydrate also represents an attractive way of storing large quantities of gas, such as hydrogen,[6] natural gas,[7,8] and carbon dioxide.[9] Extensive efforts have been carried out to develop efficient storage techniques in both the scientific and industrial fields, although to date there has been little effort to understand the physical properties of gas hydrates formed from multicomponents of natural gas, which is the major concern of this report.

Natural gas is a mixture of hydrocarbons such as methane, ethane, and propane, and a few nonhydrocarbons including hydrogen sulfide, carbon dioxide, and nitrogen. Each of these components have their own hydrate equilibriums and structural characteristics, as methane, the main component of natural gas, is known to form a structure I hydrate, but large molecules such as propane form a structure II hydrate. During the past decades, phase equilibrium studies have been conducted on various compositions of natural gas to study the hydrate stability zone for many different gas fields, and literature provides thermodynamic data and prediction software.

Recent studies with improved spectroscopic techniques provide insightful information on the structural characteristics of mixed hydrate; gas uptake measurements complemented those

* To whom correspondence should be addressed. Phone: +82-42-860-3475. Fax: +82-42-860-3134. E-mail: spkang@kier.re.kr.

10.1021/jp904994s CCC: $40.75
Published on Web 08/06/2009

spectroscopic techniques to provide the basic information including composition of hydrate phase and natural gas consumption rate. X-ray diffraction and Raman spectroscopic analysis show that structure II mixed hydrate forms from the methane and propane gas mixture; however, structure I methane hydrate forms in the next step of hydrate formation when the partial pressure of methane is above the equilibrium pressure of methane hydrate at the end of the formation of mixed hydrate.[10] A time-resolved study on hydrate formation from methane and ethane gas mixture using neutron diffraction and Raman spectroscopy suggests that the fast formation of structure II mixed hydrate is observed initially and then the transition of structure II, noted as a kinetic product, to the thermodynamically stable structure I follows.[11] For the ternary gas mixture of methane, ethane, and propane, it is suggested that the structure II mixed hydrate forms; however, a mixture of structure II and structure I hydrates is detected below the transition line, which is below the equilibrium curves.[12] Preferential enclathration of heavy hydrocarbons in the large cages of structure II hydrate has been studied by ^{13}C NMR measurement coupled with in situ Raman spectroscopy and gas uptake measurement on formation of mixed hydrate from methane, ethane, and propane gas mixture.[13] The increase of methane concentration in the vapor phase is observed possibly because of the preferential enclathration. This phenomenon, preferential occupation of natural gas components in hydrate cages, is revealed in the work of Uchida et al. by Raman observation of the hydrate formation from simulated natural gas of methane, ethane, propane, and isobutane mixture.[14] The study indicates that the larger, at least as large as isobutane, molecules reside in large cages whereas the methane molecules mainly occupy small cages of structure II, which results in the fractionation of the vapor phase. Because of the complex phase behavior during the formation of mixed hydrate from multicomponent natural gas, the structure and composition of the hydrate phase must be studied very well for industrial applications. If the composition of the vapor and hydrate phases continuously changes during the formation of hydrate because of preferential uptake of heavy hydrocarbons, it might induce the instantaneous change of structural properties with the progress of hydrate formation.[15] A computational scheme of thermodynamic simulations has been reported to follow the structure transition in the hydrate phase, which should provide important information to control the hydrate phase properties.[16]

Recently, methane hydrate formation in water-preloaded activated carbon is becoming attractive because of its potential as a storage medium of methane gas.[17] The amount of methane gas stored in a porous medium by forming hydrate seems to be close to the target value for the development of absorbed natural gas technology and the literature suggests that natural gas hydrate formation should be possible for specific activated carbons.[18] However, further investigation must be carried out with natural gas because natural gas components should exhibit different phase behavior inside micropore structures of porous media.

These results have led to the proposition that various aspects of physical chemistry have to be studied for natural gas hydrate, which can be adapted to develop hydrate-based technology for storage and transportation of natural gas. Although a large number of investigations have been carried out to identify the phase equilibrium and structural characteristics, a weak point in much of these works is that the quantitative analysis on the mixed hydrate had not been carried out or performed only at the hydrate formation temperature of near ice point, leaving the necessity of investigating the temperature effect on the preferential occupation of heavy hydrocarbons in the hydrate phase. In attempting to come to an understanding of the fractionation of the hydrate phase, we formed mixed hydrate from a multicomponent gas mixture of methane, ethane, propane, and isobutane at various temperatures, and performed the gas uptake measurements followed by hydrate phase composition analysis. ^{13}C Magic Angle Spinning (MAS) NMR spectroscopy is also used to measure the structural characteristics of mixed hydrates having single or double structures at corresponding experimental conditions. At this moment, the cage occupancy of coexisting structures for natural gas hydrate has not been widely studied. In addition, phase behavior and structural characteristics of mixed hydrate formed from water in micropore of silica gels are investigated in order to verify the effect of pore structure on the preferential occupation of heavy hydrocarbons in hydrate cages.

Experimental Section

Thermodynamic and Gas Uptake Measurements. The gas mixture used in this study was supplied by World Gas and had a UHP grade. The dry based gas composition was methane 0.8986, ethane 0.0640, propane 0.0271, and isobutane 0.0103, which simulates the natural gas composition distributed in the Korean domestic natural gas grid. HPLC grade water was supplied by Sigma-Aldrich Chemicals Co. with a purity of 99.99 mol %. Spherical silica gel particles with nominal pore diameter of 100 nm were selected and purchased from Silicycle. The properties of the silica gels were measured by mercury intrusion with Autopore VI 9500 (Micrometrics) and represented in our previous work.[19] A detailed description of the apparatus and procedure for thermodynamic measurements has been described in other works.[19,20]

The apparatus for gas uptake measurement is designed to measure the volumetric consumption rate of the gas mixture during the formation of hydrate; the apparatus consists of a semibatch reactor with a temperature-control system. The cylindrical reactor was made of 316 stainless steel and was equipped with an impeller to enhance the conversion of water to hydrate, while stirring is not used for silica gel particles. The temperature of the reactor was controlled by an externally circulating refrigerator/heater, and a K-type thermocouple probe with a digital thermometer was inserted into the reactor to measure the actual temperature of its content within an uncertainty of ± 0.05 K. The pressure of the system was measured by a digital pressure gauge of which the span was 0 to 10.0 MPa with an uncertainty of ± 0.01 MPa. A digital thermal mass flow controller (5850E, Brooks Instrument LLC) was used to obtain the amount of gas consumed during the hydrate formation, which allowed accurate measurement of the mass flow rate of the gas mixture and control of the system pressure to maintain isobaric conditions within an uncertainty of ± 5.0 cm^3/min at STP condition. A data acquisition system was used for direct gathering of temperature, pressure, and gas flow rate through the experiments. The gas composition of the vapor phase and the gas retrieved from the dissociation of hydrate phase were measured by gas chromatograph. Ice particles were prepared at 253 K by freezing liquid water; particles were finely crushed with a mortar and pestle. The water preloaded silica gels were prepared by water sorption by placing dried silica gels in a bottle with an identical amount of water with the pore volume of silica gel. After mixing, the bottle was sealed off to prevent water evaporation and was vibrated with

an ultrasonic wave at room temperature for at least 12 h to obtain complete filling of water in the pores.

The experiment for gas uptake measurement commenced with charging the reactor with prepared water phase or silica gels as we explained above. The reactor was cooled to the desired experimental temperature, and after the temperature of the reactor stabilized, a sufficient amount of natural gas was introduced into the reactor until it reached the desired experimental pressure and then maintained, which was 5.0 MPa in this study. As the gas mixture in the reactor was consumed due to the hydrate formation, the mass flow controller automatically supplied additional gas from the gas cylinder in order to maintain an isobaric condition. The composition of initial and final vapor phase composition was measured by gas chromatography, and after completion of hydrate formation, the vapor phase was discharged quickly to initiate the dissociation of the hydrate phase. The composition of the retrieved gas from the hydrate phase was measured after complete dissociation of the hydrate phase. To accurately measure the composition, we did five GC measurements and averaged the results to reduce any contamination effect. The uncertainty of GC measurement was estimated to be within ±5.0%.

NMR Spectroscopic Analysis. To determine the structural characteristics of the mixed hydrate, ^{13}C MAS NMR spectra were recorded at 243 K by placing the hydrate samples in a 4.0 mm diameter ZrO_2 rotor that was loaded into the variable temperature (VT) probe of a Bruker 400 solid state NMR spectrometer.[21,22] All spectra were recorded at a Larmor frequency of 100.6 MHz under high-power proton decoupling (HPDEC) at a spinning rate of 2−4 kHz. A pulse length of 2 μs and pulse repetition delay of 10−20 s were used with radio frequency field strengths of 50 kHz, corresponding to a 90° pulse of 5 μs duration. The downfield carbon resonance peak of adamantane, assigned a chemical shift of 38.3 ppm at 300 K, was used as an external chemical shift reference. The hydrate samples were prepared with the same apparatus and procedures as those used for gas uptake measurements. The temperature was kept at the desired experimental temperature until the natural gas consumption was completed, and the hydrate phase was sampled at liquid nitrogen temperature for ^{13}C NMR experiment.

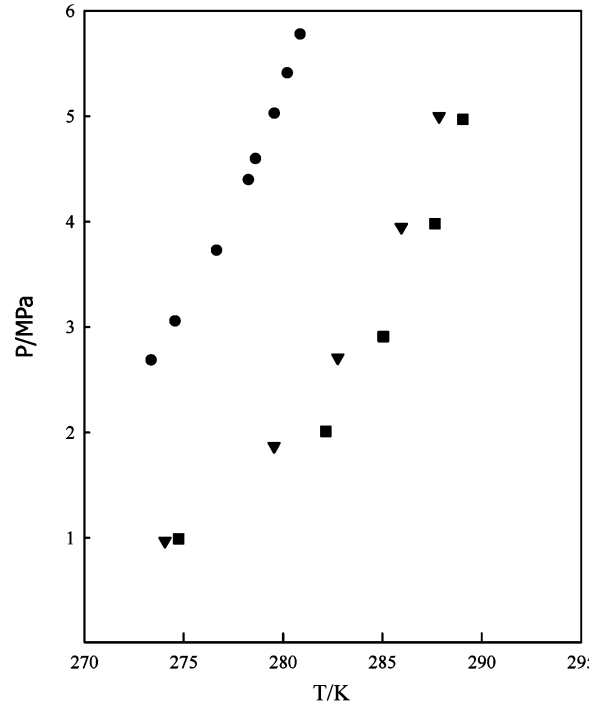

Figure 1. Hydrate phase equilibria for mixed hydrate of natural gas in bulk water (□) and in silica gel pores (▼). Solid circles (●) represent phase equilibrium conditions of pure methane hydrate in bulk water.

TABLE 1: Hydrate Equilibrium Conditions of Methane, Ethane, Propane, and Isobutane Gas Mixture in Bulk Water and in Silica Gel Pores of Nominal Diameter 100 nm

system	T (K)	P (MPa)
natural gas + bulk water	274.75	0.99
	282.15	2.01
	285.05	2.91
	287.65	3.98
	289.05	4.97
natural gas + water in silica gel pore	274.05	0.97
	279.55	1.87
	282.75	2.71
	285.95	3.95
	287.85	5.00

Results and Discussion

A large number of phase equilibrium studies have been carried out to identify three phase equilibrium conditions of hydrate (H), liquid water (L_w), and vapor (V) to give a stable region for hydrate formation. Although the P, T conditions of natural gas hydrates are represented in much of the literature, the precise measurement of the thermodynamics is needed for the corresponding composition of natural gas. An initial phase equilibrium study was carried out to measure the H−L_w−V equilibria of gas hydrate in bulk water and in silica gel pores with nominal diameter of 100 nm. The equilibrium data are shown in Figure 1 and listed in Table 1. Natural gas forms a mixed hydrate of hydrocarbon molecules and the presence of heavy hydrocarbons such as ethane and propane increases the equilibrium temperature at corresponding pressure more than that of pure methane hydrate as shown in Figure 1. The equilibrium temperature decreased in silica gel pores as it is shown that the equilibrium line is shifted to the lower temperature and higher pressure region when compared with that of the mixed hydrate from bulk water, which means that a change in the property of the mixed hydrate occurs inside the pore space. It is suggested that inside the porous media, the thermodynamic potential of the chemical components can change with respect to bulk conditions as a consequence of molecular interactions at the pore walls and the energy required to maintain capillary equilibrium.[23] The physical properties of gas hydrates from bulk water and silica gel pore water have to be analyzed, including composition, structure type, and cage occupancies.

Panels a and b of Figure 2 show gas uptake curves during the hydrate formation in bulk water and silica gel pores, respectively. The consumption of natural gas is monitored from the beginning of the experiment to observe if there is a delay in hydrate formation, i.e., induction time. As pointed out in the literature,[13] the consumed volume of natural gas as a function of time represents the conversion rate of water into hydrates, which is referred to as R_f and obtained by regressing the curves during the first 100 min after the first evidence of hydrate formation. The total consumed amount of natural gas during the formation should indicate the amount of natural gas enclathrated in cages of mixed hydrates and is explained as the value of gas-to-water ratio in this work. The gas-to-water ratio represents the volume of natural gas per unit volume of water used for hydrate formation. Table 2 represents each set of hydrate formation conditions, and the resulting driving force, conversion rate, and gas-to-water ratio.

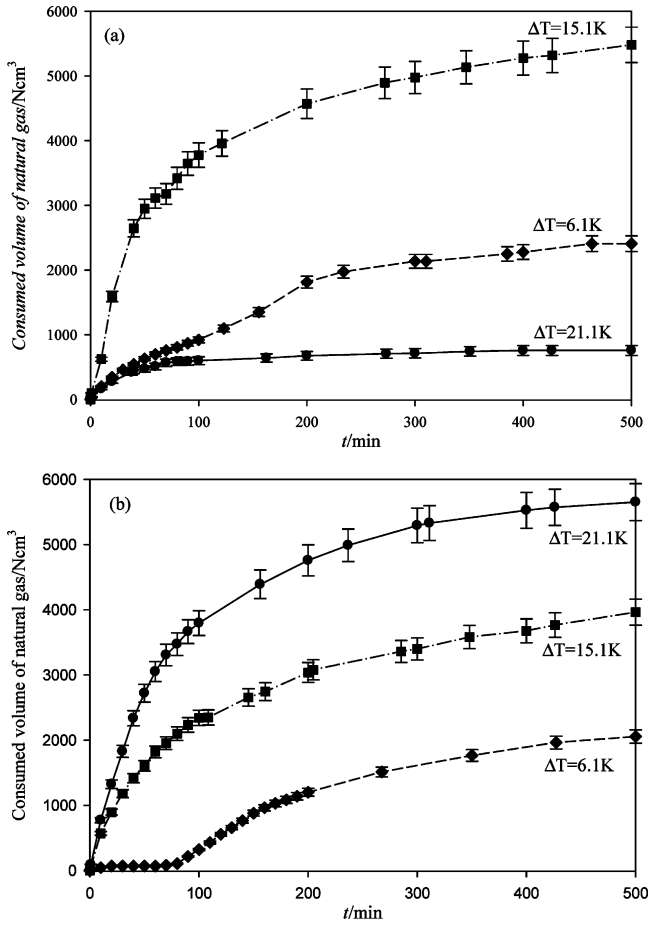

Figure 2. Gas uptake curves during the formation of mixed hydrate (a) in bulk water and (b) in silica gel pores at formation temperatures of 268.15 (●), 274.15 (□), and 283.15 K (◆).

TABLE 2: Growth Rate and Conversion Ratio from Gas Uptake Measurements at Corresponding Hydrate Formation Conditions

system	T_{exp} (K); P_{exp} (MPa)	ΔT (K)	R_f ($cm^3 \cdot min^{-1}$)	gas-to-water vol ratio (v/v)
natural gas + bulk water	268.15; 5.0	21.1	5.99	69.45
	274.15; 5.0	15.1	37.77	182.69
	283.15; 5.0	6.1	9.21	80.20
natural gas + water in silica gel pore	268.15; 5.0	19.7	37.96	188.37
	274.15; 5.0	13.7	23.43	132.12
	283.15; 5.0	4.7	10.85	68.50

For the most experimental conditions, mixed hydrate formation is observed to start instantly as soon as the stirring of the water phase commences, which means a delay of hydrate formation is negligible for formation of natural gas hydrate at studied conditions. The delay of 79 min is only observed at 283.15 K as mixed hydrate forms from water in silica gel pores of 100 nm.

As seen in Figure 2a and Table 2, for hydrate formation in bulk water, the conversion rate, R_f, increases with increasing ΔT, from 6.1 to 15.1K, but decreases with further increases of ΔT to 21.1K, at which ice particles were used as the bulk water phase. For hydrate formation in silica gel pores, the conversion rate increases with increasing ΔT as seen in Figure 2b and Table 2. Here, ΔT is defined as the temperature difference between equilibrium temperature and experimental temperature and considered as the driving force for hydrate formation. It has been quoted that the increase of driving force could result in the increase of conversion rate, which is confirmed in the case of hydrate formation in silica gel pores. However, this study suggests that the formation characteristics are also affected by the gas−hydrate interface layout. In addition, as seen in Figure 2 and Table 2, the gas-to-water ratio shows a similar trend to that of the conversion rate. It reaches 182.69 vol/vol at ΔT of 15.1 K then decreases to 69.45 v/v at ΔT of 21.1K for bulk water. However it keeps increase to 188.37 v/v for water in silica gel pores, when ΔT increases from 4.7 to 19.7 K. The values of the gas-to-water ratio were similar for both bulk water and silica gel pore water at 283.15 K. Accordingly it can be suggested that the gas-to-water ratio is directly affected by the conversion rate at the studied conditions in this work. One may explain the slow conversion of ice particles to hydrate as the hydrate shell covering ice particles acts as a barrier of mass transfer and results in early termination of hydrate formation. A more effective system to overcome the mass transfer limitation should be needed such as a fluidized bed-type reactor instead of a conventional stirred tank reactor if we use pulverized ice particles for hydrate formation.

TABLE 3: Composition of Gas Retrieved from Mixed Hydrate in Bulk Water at the Corresponding Hydrate Formation Temperature

natural gas components	feed gas	T (K)					
		268.15	270.15	274.15	276.15	278.15	283.15
CH_4	89.82	73.13	75.94	82.95	81.81	79.63	78.55
C_2H_6	6.50	12.29	11.11	10.16	11.64	12.29	12.01
C_3H_8	2.71	12.07	12.0	5.54	6.24	6.24	6.72
i-C_4H_{10}	0.97	2.51	0.95	1.35	0.31	1.84	2.72
heating value (Btu/scf)	1121.6	1341.4	1296.4	1199.4	1201.9	1238.6	1263.4

The composition of hydrate was measured by analyzing retrieved gas from mixed hydrate. The hydrate composition formed from bulk water at temperatures of 268.15 to 283.15 K is listed in Table 3 and shown in Figure 3. Initial feed gas composition is also shown in Table 3. It is confirmed that the composition of ethane and propane in the hydrate phase is higher than those in the initial feed composition at the studied temperature range, while the composition of isobutane shows a slight variation compared with the other natural gas components. As seen in Table 3 and Figure 3, the composition of retrieved gas from hydrates is different at every formation condition and each component of natural gas shows different trends which might induce complexity on physical properties of retrieved gas. Among various thermal and mechanical properties, we decided to use the heating value of retrieved gas for comparison of physical property of retrieved gas since the composition of the gas would be directly subjected to the heating value, which indicates the energy content of gas, and obtained by multiplying the composition measured by the gross heating value of each component. The gross heating values of each natural gas component can be found in the literature.[24] Moreover one of the principal uses of natural gas is as a fuel, and natural gas is normally bought and sold on the basis of its heating value, thus the heating values are calculated from the gas composition of retrieved gas at the corresponding temperature and compared to examine the extent of the fractionation in the hydrate phase. The heating value of the initial feed gas is 1121.3 Btu/scf, and the most similar heating value of the retrieved gas to that of the initial feed gas is obtained from the mixed hydrate formed at 274.15 K with a value of 1199.4 Btu/scf as seen in Table 3.

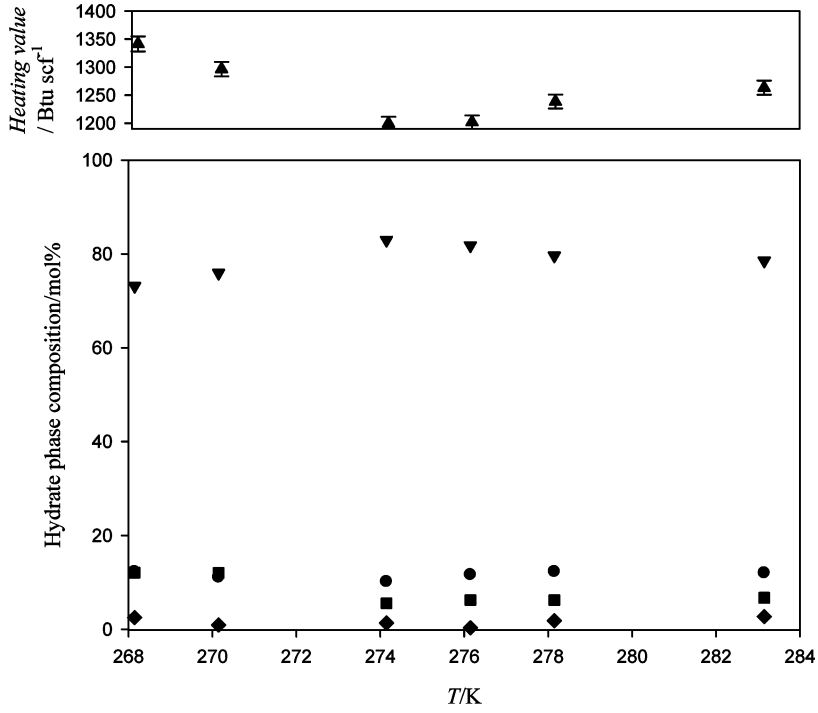

Figure 3. The composition of retrieved gas from mixed hydrate at the corresponding formation temperature in bulk water: □, methane; ▲, ethane; ▼, propane; ◆, isobutane; ●, heating value of retrieved gas from mixed hydrate.

Increasing or decreasing the temperature from 274.15 K induces the increase of the heating value because of the increase of heavy hydrocarbon contents in the retrieved gas from hydrate, and the highest heating value, 1341.4 Btu/scf, is obtained at a formation temperature of 268.15 K. Considering the formation kinetics as shown in Figure 2a and Table 2, the formation temperature of the highest heating value is the same as that of the highest gas-to-water ratio. At such temperature the composition of methane is higher than that of other formation temperatures, while the composition of ethane and propane is lower than others. Accordingly, it is expected that the composition of the hydrate phase should change during the formation of mixed hydrates and each hydrocarbon seems to have different enclathration characteristics. These results support the works in the literature on preferential uptake of heavy hydrocarbons[10,13,14] and, in addition, represent that the extent of preferential occupation is affected by the formation temperatures, resulting in a different gas-to-water ratio. We envisage that ethane and propane molecules may be captured into the hydrate phase faster than methane at early times, and at later times the enclathration of methane may become dominant due to a decrease of those compositions in the vapor phase. This explains that the methane content is high in the case of high gas-to-water ratio at 274.15 K; however, it is low in the case of low gas-to-water ratio at 268.15 K. The temperature dependence of the preferential occupation can be confirmed with both formation kinetics and hydrate composition analysis.

Figure 4 and Table 4 show the hydrate composition in the silica gel pores. The increase of heating value is observed with increasing formation temperature. The minimum heating value is 1240.2 Btu/scf at a hydrate formation temperature of 268.15 K, and different composition trends are observed from those found in bulk water. As we discussed in Figure 2b and Table 2, the decrease of formation temperature in isobaric conditions induces an increase of driving force ΔT, resulting in an increase of gas-to-water volume ratio in the silica gel pores. Again, as we discussed above, the high value of gas-to-water volume ratio indicates the high composition of methane in the hydrate phase and low heating value. We note that the composition of propane occupying cages of hydrate inside silica gel pores is about two times higher than that of hydrate formed from bulk water at a formation temperature range of 274.15 to 283.15K, resulting in about 10% increase of the heating value. For instance, the heating value of the retrieved gas from hydrate formed at 283.15 K is 1263.4 Btu/scf in bulk water, but it is 1388.5 Btu/scf in silica gel pores, although the formation conditions are the same and the kinetics show similar trends. It is known that heavy hydrocarbons are more strongly adsorbed than is methane in porous media.[25] Accordingly it is expected that the fractionation effect is enhanced in silica gel pores compared to that in bulk water. Further studies should be carried out to study this phenomenon; however, currently it is obvious that the heating value of retrieved gas from mixed hydrate is affected by the amount of captured natural gas, expressed here as gas-to-water volume ratio, and silica gel pore structures.

The ^{13}C MAS NMR experiment was carried out to analyze the structural characteristics of the mixed hydrate from natural gas. To obtain the chemical shift information of the natural gas components in hydrate cages, mixed hydrates were formed from methane/ethane and methane/ethane/propane gas mixtures. The methane and ethane gas mixture is known to show structure transition from II to I between the methane concentration range of 99.2% and 99.4% in the vapor phase.[26] In this work, mixed hydrate was formed from a 95 mol % of methane and 5 mol % of ethane gas mixture. The ^{13}C NMR spectrum is shown in Figure 5a. Previous research on hydrate structure analysis suggests that the hydrate structure can be determined from a chemical shift of methane, as it is −8.3 ppm for large cages of structure II and −6.8 ppm for large cages of structure I, while methane in small cages of both structures I and II shows a similar chemical shift at −4.3 ppm.[27] In Figure 5a, resonances of methane in hydrate cages are shown at −4.3, −6.8, and −8.3 ppm, indicating that the two hydrate structures of I and II exist together. Ethane molecules also show two resonances at 5.9

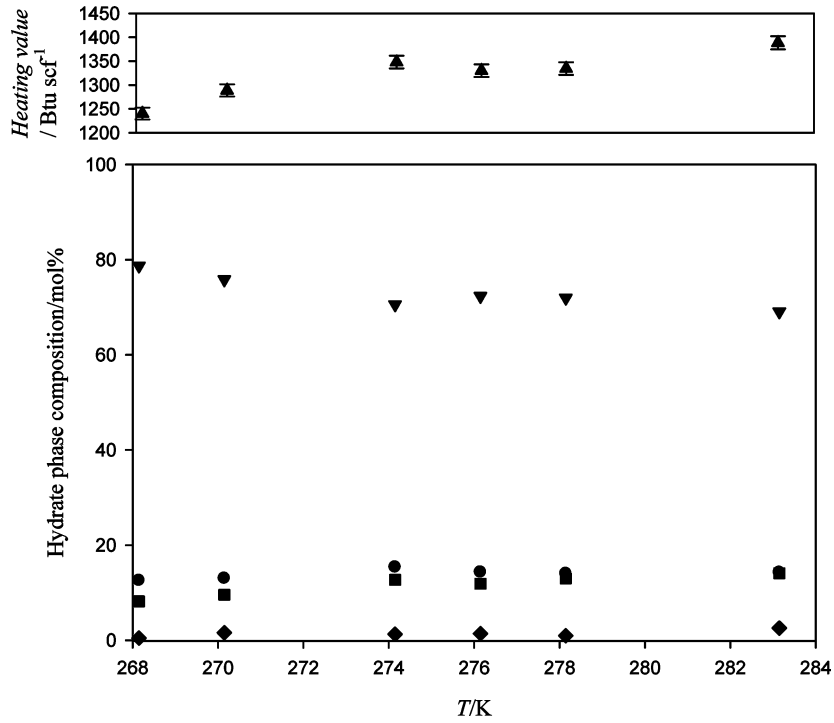

Figure 4. The composition of retrieved gas from mixed hydrate at the corresponding formation temperature in silica gel pores: □, methane; ▲, ethane; ▼, propane; ◆, isobutane; ●, heating value of retrieved gas from mixed hydrate.

TABLE 4: Composition of Gas Retrieved from Mixed Hydrate in Silica Gel Pore at the Corresponding Hydrate Formation Temperature

natural gas components	feed gas	*T* (K)					
		268.15	270.15	274.15	276.15	278.15	283.15
CH_4	89.82	78.72	75.81	70.57	72.32	71.97	69.06
C_2H_6	6.50	12.59	13.03	15.40	14.34	14.04	14.28
C_3H_8	2.71	8.19	9.57	12.70	11.91	13.01	14.11
i-C_4H_{10}	0.97	0.50	1.59	1.33	1.42	0.98	2.56
heating value (Btu/scf)	1121.6	1240.2	1288.8	1348.1	1330.1	1334.6	1388.5

and 7.6 ppm, which can be assigned to ethane in the large cages of structure I (7.6 ppm) and the large cages of structure II (5.9 ppm), respectively.[26] Figure 5b shows ^{13}C NMR spectrum when mixed hydrate was formed from a 90 mol % of methane, 5 mol % of ethane, and 5 mol % of propane gas mixture. It is known that propane molecules occupy large cages of structure II. As seen in Figure 5b, methane shows two resonances at −4.3 and −8.3 ppm, indicating that it is occupying both small and large cages of structure II. Single resonance for ethane is shown at 5.9 ppm; two distinct resonance lines for propane molecules are shown at 16.5 (−C−) and 17.3 ppm (C−). Accordingly, for this composition of gas mixture, it can be concluded that mixed hydrate has structure II and that the small cages are occupied by methane molecules, while large cages are shared by methane, ethane, and propane molecules. Panels a and b of Figure 5 show that the methane and ethane gas mixture could form different types of hydrate structures depending on the composition of the vapor phase; however, the presence of propane should induce the formation of structure II only and suppress the formation of structure I. On the basis of these results, ^{13}C NMR spectra for mixed hydrate formed from natural gas, i.e., gas mixture of methane, ethane, propane, and isobutane, were analyzed to obtain the physical properties of structure type and cage occupancies.

Figure 6a shows ^{13}C NMR spectrum of mixed hydrate formed from reaction of natural gas with bulk water at 274.15 K and 5.0 MPa, as its gas uptake measurement has been shown in Figure 2a. Methane molecules occupied both small and large cages of structure II; there is no sign of structure I. Ethane molecules show a single resonance line at 5.9 ppm; propane shows two resonance lines at 16.5 and 17.3 ppm, indicating they occupied a certain number of large cages of structure II. For isobutane, it is expected that two resonance lines should be raised; however, a broad resonance line at 26.3 ppm is shown because of the small number of butane molecules that are expected to occupy part of the large cages of structure II, as seen in the hydrate phase composition of Table 3. The cage occupancies of natural gas components are calculated from the ratio of integrated intensity of NMR signals at each chemical shift with the following thermodynamic equation that describes the cage occupancies of guest molecules with the chemical potential of structure II,

$$\mu_w(h) - \mu_w(h^o) = \frac{RT}{17}[\ln(1 - \theta_{L,C_4H_{10}} - \theta_{L,C_3H_8} - \theta_{L,C_2H_6} - \theta_{L,CH_4}) + 2\ln(1 - \theta_{S,CH_4})] \quad (1)$$

where $\mu_w(h^o)$ is the chemical potential of water molecules of a hypothetical empty lattice and θ_S and θ_L the fractional occupancy of small and large cages, respectively. When the hydrate is in equilibrium with ice, the left side of eq 1 becomes $\mu_w(\text{ice}) - \mu_w(h^o) = -\Delta\mu_w^o$, where $\Delta\mu_w^o$ is the chemical potential of the empty lattice relative to ice. The value of $\Delta_r\mu_w^o(h^o)$ used in eq 1 was 883.8 J/mol, because this value corresponds to structure II. The ^{13}C MAS NMR spectra in Figure 6a provide the integrated intensity ratio of methane to ethane, propane, and butane molecules, which then can be used to calculate the cage occupancies of each molecule from eq 1. Results are presented as cage occupancies in Table 5. As we pointed out, small cages are only occupied by methane molecules in cage occupancy of 0.78; large cages are shared by methane, ethane, propane, and isobutane molecules. The occupancies of each molecule are 0.68,

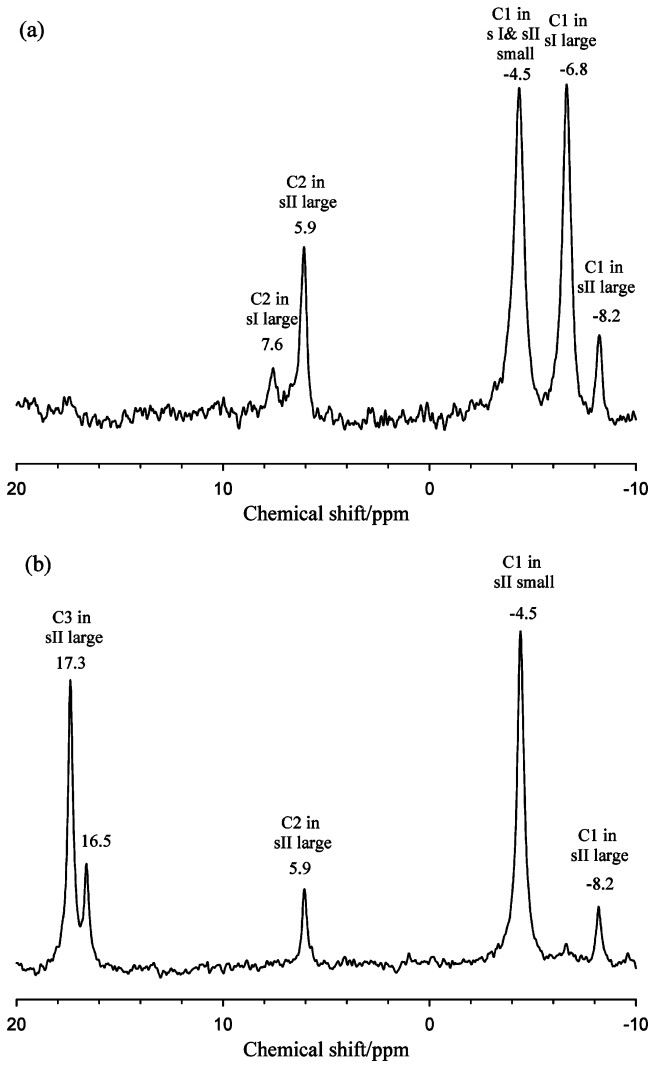

Figure 5. ^{13}C MAS NMR spectra for mixed hydrates from (a) methane and ethane gas mixture and (b) methane, ethane, and propane gas mixture.

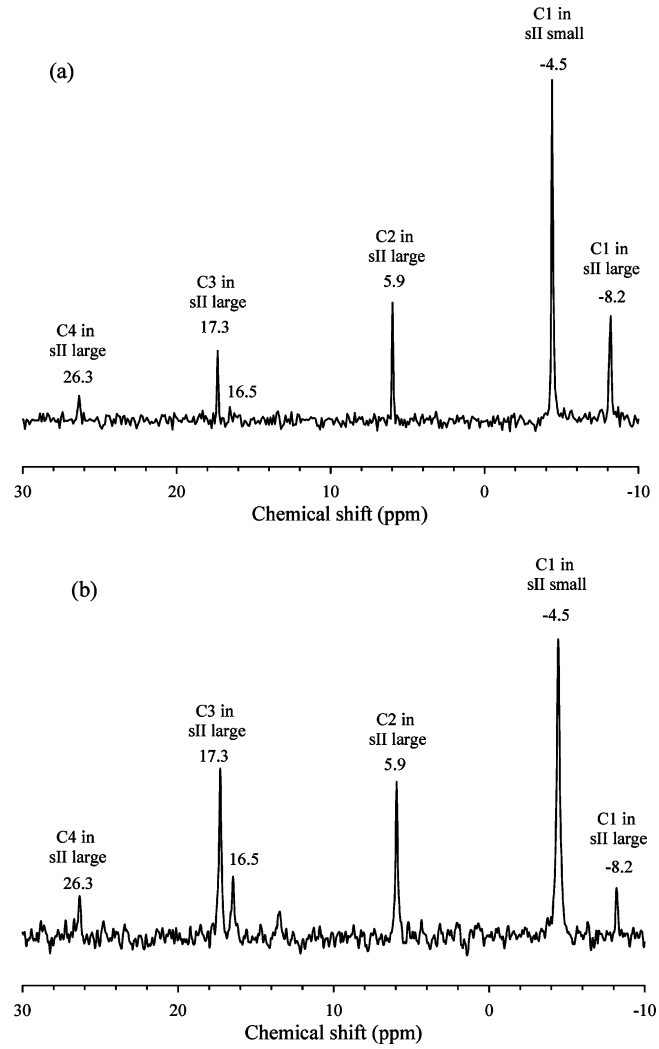

Figure 6. ^{13}C MAS NMR spectra for mixed hydrates from natural gas (a) in bulk water and (b) in silica gel pores.

0.18, 0.08, and 0.02, respectively, suggesting that about 68% of large cages are occupied by methane molecules. The hydrate composition based on the cage occupancy calculation is similar to those of the gas uptake measurements, thus confirming the high composition of methane in the hydrate phase as discussed in Figure 3. Figure 6b shows ^{13}C NMR spectra of mixed hydrate in silica gel pores formed at 274.15 K and 5.0 MPa as its gas uptake measurement has been shown in Figure 2b. Overall resonance lines show a similar trend to those of Figure 6a, indicating that only structure II is formed. However, the ratio of integrated intensities gives a lot of different cage occupancies compared with those of mixed hydrate in bulk water. For small cages, the occupancy of methane increases to 0.87; for large cages the occupancy of methane decreases dramatically to 0.19. Instead, the occupancy of ethane and propane molecules increased to 0.33 and 0.36, respectively. We note that the cage occupancy of propane in large cages of hydrate formed from water in silica gel pores increases almost four times higher than that of propane in large cages of hydrate formed from bulk water, confirming the trend of propane composition increase in the hydrate phase as discussed in the hydrate composition analysis of Figures 3 and 4. The ethane and propane molecules are bigger than the methane molecules; however, it is likely that those heavy hydrocarbons prefer to be transported inside silica gel pores and to participate in the formation of mixed hydrate by occupying a large number of structure II large cages as evidenced by ^{13}C NMR spectra. The gas uptake measurement and ^{13}C NMR analysis suggest that although feed gas composition and formation conditions are identical for hydrate formation in bulk water and silica gel pores, the resulting mixed hydrate can exhibit different cage occupancies because of different gas−water interface reaction in confined pore structure.

Now it is obvious that the preferential occupation of heavy hydrocarbons results in the fractionation of the hydrate phase. Considering the relationship between the gas-to-water volume ratio and the hydrate composition, it is presumed that the enclathration kinetics of each natural gas component would be different according to corresponding formation environments. The results of the hydrate composition and ^{13}C NMR analysis suggest that the enclathration of propane molecules is faster than that of methane at the early stage of the formation of mixed hydrate; however, at a later stage of hydrate formation the enclathration of methane molecules is likely to be dominant due to the enrichment of the vapor phase with methane. The composition analysis shows that methane composition in the vapor phase keeps increasing with the proceeding of the mixed hydrate formation and reaches 96−98 mol % after completion of hydrate formation. If methane becomes rich in the vapor phase and heavy hydrocarbons are not supplied, the hydrate formation may proceed to a different structure, i.e., structure I.

TABLE 5: Cage Occupancies of Natural Gas Components in the Corresponding Cages of Hydrate Structures

		CH_4		C_2H_6	C_3H_8	i-C_4H_{10}
system	structure	$\theta_{S,C1}$	$\theta_{L,C1}$	$\theta_{L,C2}$	$\theta_{L,C3}$	$\theta_{L,C4}$
natural gas + bulk water[a]	structure II	0.78	0.68	0.18	0.08	0.02
natural gas + water in silica gel pore	structure II	0.87	0.19	0.33	0.36	0.04
natural gas + bulk water[b]	structure II	0.75	0.70	0.18	0.06	0.02
	structure I	0.76	0.93			

[a] Mixed hydrate is formed in semibatch process. [b] Mixed hydrate is formed in batch process.

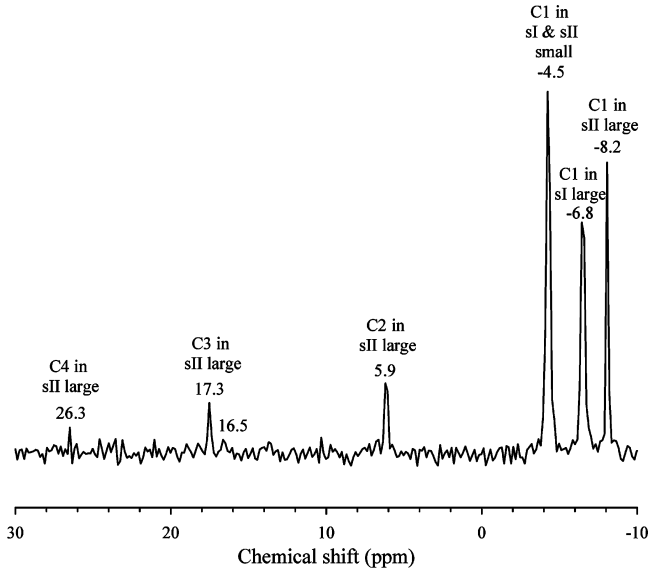

Figure 7. ^{13}C MAS NMR spectra of coexisting structure II mixed hydrate and structure I methane hydrate.

To investigate the effect of vapor phase composition variation, a mixed hydrate is formed by using a batch-type process, in which hydrate formation proceeds without supplying fresh natural gas to maintain isobaric conditions. At 274.15 K, the system pressure reaches 4.2 MPa from 5.0 MPa after completion of hydrate formation, and the resulting ^{13}C NMR spectrum of mixed hydrate is shown in Figure 7. Ethane, propane, and isobutane molecules all occupied the large cages of structure II, as seen in the resonance lines at corresponding chemical shifts. However, methane molecules show more complicated resonances at −6.8 ppm for large cages of structure I and −8.3 ppm for large cages of structure II. Resonance lines of methane molecules in small cages of structures I and II are not distinguished in the spectra; this shows a chemical shift of −4.3 ppm. To calculate the cage occupancies of the methane molecules, the results from our previous work have been used. The following thermodynamic equation has been used to calculate the cage occupancies of methane in cages of structure I,

$$\mu_w(h) - \mu_w(h^o) = \frac{RT}{23}[3\ln(1 - \theta_{L,CH_4}) + \ln(1 - \theta_{S,CH_4})] \quad (2)$$

The value of $\Delta\mu_w^o(h^o)$ used in eq 2 was 1297 J/mol for a structure I hydrate. Its small cages are occupied by methane molecules in cage occupancy of 0.76; large cages are occupied in cage occupancy of 0.93, suggesting that most of the large cages are occupied by methane molecules without evidence of ethane molecules. It is noted that the occupancy of structure II formed in the batch process is similar to those values of structure II formed in the semibatch process, as seen in Table 5. The integrated intensity ratio of methane in structure I is used together with the integrated intensity ratio of methane and other hydrocarbons in structure II to calculate the ratio of hydrocarbons in both hydrate structures. This gives the ratio of hydrocarbons in structure II to those in structure I as 0.72, indicating that 72% of hydrocarbons in the hydrate phase are occupying the cages of structure II and 28% of hydrocarbons in hydrate phase are occupying the cages of structure I. It is expected that during the formation process the initial hydrate structure should be structure II because of sufficient heavy hydrocarbons in the vapor phase; however, at a certain point structure I methane hydrate started to form because the partial pressure of heavy hydrocarbons in the vapor phase was no longer enough to form structure II. It is also noted that during the formation of structure I methane hydrate, ethane molecules do not participate in its formation and remain in the vapor phase.

More precise studies should be carried out, such as in situ study of the formation process; however, we note that the formation of mixed hydrate from natural gas shows complex characteristics because of preferential occupation of heavy hydrocarbons. This complexity needs to be explored for development of a chemical process for natural gas storage and transportation in hydrate form. As discussed before, since the value of commercial natural gas is based on its heating value, the control of hydrate phase composition might become a key variable in the design of the process. It is clear that studies of hydrate composition and structural characteristics of mixed hydrates, as reported here, will offer important design parameters for the chemical process for natural gas storage and transportation in hydrate form.

Conclusions

We have shown that heavy hydrocarbon molecules of natural gas occupy preferentially large cages of structure II during the formation of mixed hydrate, resulting in the fractionation of the hydrate phase. High driving force, ΔT, induced high conversion of water molecules into hydrate in overall experimental conditions, although at 268.15 K in bulk water, a low conversion ratio was observed because of hydrate shell on the surface of ice particles. The heating value of the retrieved gas from mixed hydrate is similar to that of the initial feed gas at a temperature of 274.15 K in bulk water and 268.15 K in silica gel pores. The composition analysis suggests that the enclathration of heavy hydrocarbon molecules might be faster than that of light methane molecules at the early stage of the hydrate formation process. We use ^{13}C MAS NMR to analyze structure type and guest molecule distribution over the cage sites. Indeed, it is observed that the structure II mixed hydrate is formed from natural gas and heavy hydrocarbon molecules occupy large cages more preferentially, resulting in an increase in the heating value of the retrieved gas from mixed hydrate. We note that the formation of mixed hydrate in silica gel pores enhanced the fractionation of heavy hydrocarbon molecules, as 73% of

large cages are occupied by ethane, propane, and isobutane molecules, while methane molecules occupy only 19% of large cages of structure II. The enrichment of the vapor phase with methane might induce structural transition, and the coexisting structures II and I are observed when mixed hydrate forms in the batch process. The ratio of hydrocarbons in structure II to those in structure I is 0.72, suggesting that structure I can be formed at a later stage of the hydrate formation process when the vapor phase is sufficiently enriched with methane. Although there are still a number of features to be explored, the preferential occupation of heavy hydrocarbon molecules will be one of the important characteristics that have to be investigated carefully to develop natural gas storage and transportation processes by synthesis of mixed hydrate.

Acknowledgment. The authors would like to acknowledge funding from the Korea Ministry of Knowledge Economy (MKE) through the "Energy Technology Innovation Program". This work was also partially supported by the Korea Institute of Energy Research.

References and Notes

(1) Sloan, E. D., Jr., Koh, C. *Clathrate Hydrates of Natural Gases* 3rd ed.; CRC Press: Boca Raton, FL, 2008.
(2) Sinquin, A.; Arla, D.; Prioux, C.; Peytavy, J. L.; Glenat, P.; Dicharry, C. *Energy Fuels* **2008**, *22*, 721.
(3) Sloan, E. D., Jr. *Nature* **2003**, *426*, 353.
(4) Milkov, A. V.; Sassen, R. *Mar. Pet. Geol.* **2002**, *19*, 1.
(5) Kvenvolden, K. A. *Chem. Geol.* **1988**, *71*, 41.
(6) Lee, H.; Lee, J.-W.; Kim, D. Y.; Park, J.; Seo, Y.; Zeng, H.; Moudrakovski, I. L.; Ratcliffe, C. I.; Ripmeester, J. A. *Nature* **2005**, *434*, 743.
(7) Kobayashi, T.; Imura, N.; Ohmura, R.; Mori, Y. H. *Energy Fuels* **2007**, *21*, 545.
(8) Takahashi, M.; Moriya, H.; Katoh, Y.; Iwasaki, T. Proceedings of the 6th International Conference on Gas Hydrates, Vancouver, Canada, July 6−10, 2008.
(9) Tajima, H.; Yamasaki, A.; Kiyono, F. *Energy Fuels* **2004**, *18*, 1451.
(10) Uchida, T.; Moriwaki, M.; Takeya, S.; Ikeda, I. Y.; Ohmura, R.; Nagao, J.; Minagawa, H.; Ebinuma, T.; Narita, H.; Gohara, K.; Mae, S. *AIChE* **2004**, *50*, 518.
(11) Murshed, M. M.; Kuhs, W. F. *J. Phys. Chem. B* **2009**, *113*, 5172.
(12) Schicks, J. M.; Naumann, R.; Erzinger, J.; Hester, K. C.; Koh, C. A.; Sloan, E. D., Jr. *J. Phys. Chem. B* **2006**, *110*, 11468.
(13) Kumar, R.; Linga, P.; Moudrakovski, I. L.; Ripmeester, J. A.; Englezos, P. *AIChE* **2008**, *54*, 2132.
(14) Uchida, T.; Takeya, S.; Kamata, Y.; Ohmura, R.; Narita, H. *Ind. Eng. Chem. Res.* **2007**, *46*, 5080.
(15) Tsuji, H.; Kobayashi, T.; Okano, Y.; Ohmura, R.; Yasuoka, K.; Mori, Y. H. *Energy Fuels* **2005**, *19*, 1587.
(16) Ogawa, H.; Imura, N.; Miyoshi, T.; Ohmura, R.; Mori, Y. H. *Energy Fuels* **2009**, *23*, 849.
(17) Zhou, Y.; Wang, Y.; Chen, H.; Zhou, L. *Carbon* **2005**, *43*, 2007.
(18) Najibi, H.; Chapoy, A.; Tohidi, B. *Fuel* **2008**, *87*, 7.
(19) Kang, S.-P.; Lee, J.-W.; Ryu, H.-J. *Fluid Phase Equilib.* **2008**, *274*, 68.
(20) Seo, Y.; Kang, S.-P.; Lee, S.; Lee, H. *J. Chem. Eng. Data* **2008**, *53*, 2833.
(21) Seo, Y.; Lee, H. *J. Phys. Chem. B* **2004**, *108*, 530.
(22) Seo, Y.; Lee, H.; Koran, *J. Chem. Eng.* **2003**, *20*, 1085.
(23) Seo, Y.; Lee, H.; Uchida, T. *Langmuir* **2002**, *18*, 9164.
(24) Kidnay, A. J.; Parrish, W. *Fundamentals of natural gas processing*; Dekker mechanical engineering series; CRC/Taylor & Francis: Boca Raton, FL, 2006.
(25) Mota, J. P. *AIChE* **1999**, *45*, 986.
(26) Subramanian, S.; Ballard, A. L.; Kini, R. A.; Dec, S. F.; Sloan, E. D. *Chem. Eng. Sci.* **2000**, *55*, 5763.
(27) Seo, Y.; Lee, H.; Moudrakovski, I. L.; Ripmeester, J. A. *ChemPhysChem* **2003**, *4*, 379.

JP904994S